research articles Journal of proteome research

Doxorubicin-Induced Thymus Senescence

Rukhsana Sultana,*,†,▽,○ Fabio Di Domenico,‡ Michael Tseng,§ Jian Cai,|| Teresa Noel,⊥ R. Lakshman Chelvarajan, William D. Pierce,|| Ciara Cini,‡ Subbarao Bondada,# Daret K. St. Clair,⊥ and D. Allan Butterfield*,†,▽,○

Department of Chemistry, University of Kentucky, Lexington, Kentucky 40506, United States, Department of Biochemical Sciences, Sapienza University of Rome, 00185 Rome, Italy, Department of Anatomical Sciences & Neurobiology, University of Louisville, Louisville, Kentucky 40202, United States, Department of Pharmacology, University of Louisville, Louisville, Kentucky 40202, United States, Department of Toxicology, University of Kentucky, Lexington, Kentucky 40536, United States, Department of Microbiology, Immunology and Molecular Genetics, University of Kentucky, Lexington, Kentucky 40536, United States, Center of Membrane Sciences, and Sanders-Brown Center on Aging, University of Kentucky, Lexington, Kentucky 40506, United States

Received May 14, 2010

Doxorubicin (DOX) is an anticancer drug used for the treatment of solid tumors. The ability of DOX to treat cancer is not specific to cancer cells; some of the cells that are normal may also become targets of DOX, thereby altering the normal cellular functions and eventual cell loss. DOX effects have been studied in detail in heart because of its ability to cause cardiomyopathy. The exact mechanism of DOX-induced cardiomyopathy is not completely understood. One of organs that can be affected by DOX is thymus. DOX treatment leads to degeneration of thymus; however, since thymus undergoes age-dependent degeneration, researchers have understudied the effect of DOX on thymus. In the present investigation, we studied the effects of DOX on thymus, an organ that is important for the T-cell maturation. DOX treatment led to loss of cortical cells, decrease lymphopoiesis and increased the number of Hassells corpuscles, a marker of thymus aging. Proteomics analysis led to identification of a number of thymic proteins whose expression are altered by in vivo DOX treatment. Taken together, these results are consistent with the notion that DOX-treatment leads to thymic senescence.

Keywords: Doxorubicin • thymus • proteomics • ultrastructure • senescence

Introduction

Doxorubicin (DOX), commonly referred to as adriamycin, is an anticancer drug used for the treatment of solid tumors. The anticancer activity of the DOX has been explained by its ability to intercalate into DNA,[1−3] inhibit topoisomerase II,[4] and increase the production of reactive oxygen species (ROS).[5,6] These mechanisms are not specific to cancer cells; indeed, some normal cells may also become a target of DOX, thereby altering normal cellular functions. The effects of DOX treatment have been studied in detail in heart because of its ability to cause cardiomyopathy. The exact mechanism of the DOX-induced cardiomyopathy is not completely understood, but several studies showed that DOX can induce mitochondrial impairment, which may leads to increase release of free radicals in addition to altered cellular energetics.[7,8] In fact, DOX-induced cardiotoxicity limits the dosage and frequency by which DOX can be administered to treat solid tumors. Previous studies from our laboratory and others have showed that DOX treatment leads to increased oxidative stress *in vivo* in brain,[9−11] testes,[12] kidneys,[13] liver,[13] and plasma.[14,15] However, no studies have been conducted so far on the effect of DOX on thymus.

Thymus undergoes an age-dependent degeneration that occurs during normal human aging leading to generalized deterioration of immune functions. This, in turn, affects all cells and organs of the innate and adaptive immune systems, a process referred to as "immunosenescence". Immunosenescence leads to increase susceptibility of an individual to infections as well as increased incidence of autoimmune phenomena and cancer in the elderly.[16−18] The mechanisms that underline involution of the thymus are not well understood.

This current study is the first to show that DOX treatment leads to degeneration of thymus. However, since thymus undergoes an age dependent degeneration, the effects of DOX on thymus have been largely ignored. Given that DOX is given to children who still need a functional thymus for T-cell maturations and to build a pool of memory cells to fight with

* To whom correspondence should be addressed. Dr. Rukhsana Sultana, Department of Chemistry, University of Kentucky, Lexington, KY 40506, USA. Phone, 859-257-3615; fax, 859-257-5876; e-mail, rsult2@uky.edu. Prof. D. Allan Butterfield, Department of Chemistry, Center of Membrane Sciences, and Sanders-Brown Center on Aging, University of Kentucky, Lexington, KY 40506, USA. Phone, 859-257-3184; fax, 859-257-5876; e-mail, dabcns@uky.edu.

† Department of Chemistry, University of Kentucky.

▽ Center of Membrane Sciences, University of Kentucky.

○ Sanders-Brown Center on Aging, University of Kentucky.

‡ Sapienza University of Rome.

§ Department of Anatomical Sciences & Neurobiology, University of Louisville.

|| Department of Pharmacology, University of Louisville.

⊥ Department of Toxicology, University of Kentucky.

Department of Microbiology, Immunology and Molecular Genetics, University of Kentucky.

10.1021/pr100465m

Published on Web 10/14/2010

disease causing microbes, the effects of DOX on thymus is critical. Humans live in an environment where challenges from microbes is ongoing, and having a thymus with impaired or decrease functions will lead to decrease ability to fight infection. A dysfunctional thymus may lead to compromised immune system, which together with the additive side effect of the anticancer drug, may compromise the life of the person with cancer. Even in case of adults in whom the thymus is reduced extensively, but has some functional tissue even at an older age, thymus is important for T-cell maturation to promote a healthy life.

The above considerations have provided the rationale for the current study of the role of DOX on thymus. We used proteomics approach to identify thymic proteins of altered levels associated with DOX-induced thymic senescence. In this paper, we report that DOX-treatment leads to thymic senescence characterized by reduced size, weight, and loss of thymus cells. Further, our proteomics approach identified a number of proteins with altered levels in DOX-treated thymus, which may have relevance to immunosenescence.

Experiments

Material. Doxorubicin HCl (DOX) was purchased from Bedford Laboratories (Bedford, OH). All other chemicals were purchased from Sigma-Aldrich (St. Louis, MO), unless stated otherwise.

Methods.

DOX-Treatment. Male B6C3 mice (approximately of 3 months of age), weighing 30 g were housed in the University of Kentucky Central Animal Facility in 12 h light/dark conditions and fed standard Purina rodent laboratory chow ad libitum. The animal protocol used in this study was approved by the University of Kentucky Animal Care and Use Committee. DOX (25 mg/kg body weight) was administered intraperitoneally (ip) to six mice, while the other the six mice received saline injections. Animals were anesthetized with sodium pentobarbital after 72 h and perfused with saline followed by isolation of thymus.

Cytological and Ultrastructural Analysis. Thin slices of thymus from all samples were cut and dissected into 3 mm^3 pieces, postfixed in 2% osmium tetraoxide, dehydrated in ascending ethanol, and embedded in Araldite 502. Polymerized blocks were cut at 1 um thickness stained with Toluidine blue for light microscopy analysis. Thin sections were made, double stained with uranyl acetate and lead citrate before examined in a Philips CM 10 electron microscope operated at 60 kV.

Flow Cytometric Analyses. mAbs were purchased from BD Biosciences (San Jose, CA). The stained cells were analyzed on a FACScan flow cytometer (Becton Dickinson, Mountain View, CA). For each sample, at least 3×10^5 cells, gated on a combination of forward (FSC) and side (SSC) scatter, were acquired.

Preparation of Thymus Homogenate. Thymus tissues were collected and homogenized into an ice-cold lysing buffer (4 μg/mL leupeptin, 4 μg/mL pepstatin, 5 μg/mL aprotinin, 2 mM ethylenediaminetetraacetic acid, 2 mM ethylene glycol-bistetraacetic acid, and 10 mM 4-(2-hydroxyethyl)-1-piperazine-ethanesulfonic acid (pH 7.4)) to obtain a final 20% homogenate. Homogenates were centrifuged at 2000*g* for 10 min and the pellets containing unbroken cells or cell debris were discarded. The supernatants were used for the current studies.[19] The protein contents in the samples were determined using the BCA method (Pierce, Rockford, IL).

Proteomics. We have previously used proteomics to identify differentially expressed and oxidatively modified proteins in brain tissue of Alzheimer's disease, an age-related neurodegenerative disease.[20−22] In this study, we used proteomics as a tool to identify proteins that shows differential levels upon DOC treatment.

To the thymus homogenates (150 μg), ice-cold 100% tricholoroacetic acid (TCA) was added to a final concentration of 15% TCA and incubated on ice for 10 min. Samples were centrifuged at 14 000*g* for 5 min at 4 °C, and precipitates were washed with 0.5 mL of 1:1 ethanol/ethyl acetate (v/v) 4 times by centrifugation at 14 000*g* for 3 min at 4 °C. The protein pellets were then reconstituted in 200 μL of a rehydration buffer (8 M urea, 2 M thiourea, 50 mM dithiothreitol, 2% (w/v) CHAPS, 0.2% (v/v) Biolytes, and bromophenol blue) and loaded on the pH 4−7 ReadyIPG Strips (Bio-Rad, Hercules, CA). After 1 h, 2 mL of mineral oil was added followed by active rehydration at 50 V for 16−18 h. This was then followed by IEF of the proteins as follows: 300 V for 1 h, a linear gradient to 8000 V for 5 h and finally, 20 000 V for 1 h. Focused strips were stored at −80 °C until the second dimension of gel electrophoresis was performed.

For sodium dodecyl sulfate (SDS) PAGE, IPG strips were thawed at room temperature followed by equilibration for 15 min in a buffer containing 50 mM Tris-HCl (pH 6.8), 6 M urea, 1% (w/v) SDS, 30% (v/v) glycerol, and 0.5% dithiothreitol (DTT). Next, IPG strips were reequilibrated in the same buffer containing 4.5% iodoacetamide rather than DTT. Strips were placed into Linear Gradient (8−16%) Precast Criterion Tris-HCl gels (Bio-Rad, Hercules, CA) and run at 200 V for ∼65 min.

SYPRO Ruby Staining. Following electrophoresis, gels were removed and placed in fixing solution [7% acetic acid (v/v), 10% methanol (v/v), in water] for 45 min on a rocker, followed by overnight incubation of the gels in 50 mL of SYPRO Ruby fluorescent gel stain (Bio-Rad, Hercules, CA). SYPRO Ruby was then removed and gels were stored in deionized water.

Image and Statistical Analysis. SYPRO Ruby-stained gels were scanned using a STORM phosphoimager (Molecular Dynamics, Sunnyvale, CA) at excitation and emission wavelengths of 470 and 618 nm, respectively, and images were saved as a TIFF file. PD-Quest (Bio-Rad, Hercules, CA) imaging software was then used to match and align protein spots across the gels from the control and DOX-treated groups. Protein spots were normalized to the total density detected in each individual gel image. Proteins were considered to be statistically different between treatment groups based on a ≥1.5-fold-change and a p-value <0.05 (using a Student's t test).

In-Gel Trypsin Digestion. Protein spots of showing statistically significant difference were excised from SYPRO Ruby-stained gels with a clean blade and transferred into a 0.5 mL Eppendorf microcentrifuge tube. Excised gel pieces were washed with 0.1 M NH_4HCO_3 buffer at room temperature for 15 min. Acetonitrile (ACN) was added and allowed to incubate for 15 min. The mixed solution was removed and the gel pieces were allowed to dry in the tubes for 30 min. Next, gel pieces were incubated with 20 mM DTT in 0.1 M NH_4HCO_3 at 56 °C for 45 min. The DTT solution was removed and gel pieces were incubated with 55 mM iodoacetamide in 0.1 M NH_4HCO_3 for 15 min. The solution was removed and gel pieces were incubated with 50 mM NH_4HCO_3 for 15 min, followed by the addition of ACN for 15 min. This mixed solution was removed and gel pieces were allowed to dry for 30 min. A solution of 20 ng/μL modified trypsin (Promega, Madison, WI) in 50 mM

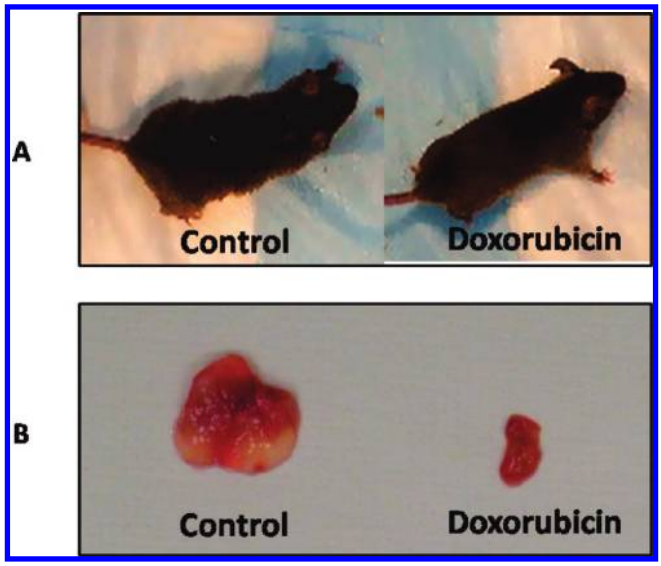

Figure 1. Mice treated with doxorubicin and controls are shown in panel A. Mice treated with doxorubicin showed reduced thymus size (B) compared to controls.

NH_4HCO_3 was added to gel pieces in order to submerge them and were allowed to shake overnight at 37 °C.

Mass Spectrometry and Database Searching. Tryptic digests were removed from gel pieces and transferred to a new microcentrifuge tube. Additional tryptic peptides were extracted from gel pieces by addition of 5 mM NH_4HCO_3 for 10 min with sonication. Next, 95% ACN in 1 mM NH_4HCO_3 was added for another 10 min with sonication. This supernatant was combined with the previous tryptic solution and concentrated to a small volume (~10 μL). C18 ZipTips (Millipore, Billerica, MA) were used to remove salts from samples prior to MS analysis. Samples were loaded into a 96-well plate rack for nanoelectrospray infusion using an Advion Tri-Versa Nanomate (Ithaca, NY). Electrosprayed peptides were analyzed with an LTQ-Orbitrap XL (ThermoScientific, Waltham, MA) mass spectrometer. The Orbitrap was set to acquire a full MS scan at 60 000 resolution and in Data Dependent mode the eight most intense ions were selected for fragmentation and mass analyzed in the Orbitrap at 30 000 resolution. Conditions for fragmentation in the ion trap include a normalized collision energy of 35%, activation time of 30 ms, and selection of only +2 charge states or higher. Total acquisition time was 5 min per sample. SEQUEST was used for database searching against the Uniprot Swiss-Prot Database and the International Protein Index (IPI) Mouse Database. Filter criteria of returned protein lists included protein probabilities <0.01, peptide XCorr values >1.5 (for +1 charge state), 2.0 (+2 charge state), 2.5 (+3 charge state), and 3.0 (+4 charge state), peptide ΔCN values >0.1, and at least 2 peptides identified for each protein. Protein MW and p*I* information was also used to assess individual protein identifications based on the location of the excised protein spot from the 2D gel. Only protein spots assigned to a single protein were further considered.

Results

Figure 1 shows control and DOX-treated mice (Figure 1A) and isolated thymus (Figure 1B). Mice treated with DOX showed a decrease in total body weight and also thymus weight (Table 1, Figure 1). Further, the mice treated with DOX showed reduced size of the thymus which suggests the loss of a number of cells from thymus upon DOX treatment. Light microscopic examination of the thymus revealed decreased number of cortical cells in DOX-treated group compared to the controls (Figure 2A,B). Thymus of the control mice showed normal cytoarchitecture with an abundance of lymphocytes and thymocytes. Few thymocytes formed cytoplasmic canaliculi containing floccular material. Hassell's corpuscles were irregularly shaped with the surrounding epitheloid cell (Figure 2A). DOX-treated samples, in contrast, showed a decrease in lymphocyte and a large number of vesiculated thymocytes (Figure 2B). Ultrastructure of the controls showed the normal array of lymphocytes, thymocytes, and numerous large macrophages (Figure 2C). The latter contained some lysosomes along with a typical array of organelles including numerous mitochondria (Figure 2D). As seen by light microscopy, DOX treatment for 3 days showed continuing lymphocytopoiesis. Clusters of lymphocytes with large ovoid shaped nuclei and a thin rim of cytoplasm were commonly observed (Figure 2E). Perivascular space contained mobile cells of defense including plasma cells, eosinophils, and macrophages. Hassel's corpuscle became irregular and the surrounding epithelial thymocytes displayed bundles of tonofibers with patches of anchoring desmosomes (Figure 2F). Other noticeable changes were found to occur in the large thymocytes endowed with cytoplasmic vascules and lipid droplets (Figure 2G). One known DOX effect on mitochondria which is a consistently found is the degenerating mitochondria in varying stages of being incorporated into the phagolysosomes (Figure 2G, inset). Beyond these changes, some thymocytes have degenerated with pyknotic nuclei and fragmenting organelles (Figure 2H).

Table 1. Doxorubicin Treatment Leads to Loss of Body and Thymus Weights

weights	control (mean ± SD)	DOX (mean ± SD)
Body weight (mg, % weight loss)	2.1 ± 1.1	10.7 ± 1.4[a]
Thymus weight (mg)	37 ± 1.5	12 ± 1.3[a]

[a] $p < 0.05$, $n = 6$.

Further, to determine if DOX treatement interfered with thymic lymphopoiesis, the thymic cells were obtained from both control and DOX mice and subjected to flow cytometry. Mice treated with DOX showed a significant decrease in the number of thymocytes. During T cell development, $CD4^-CD8^-$ double negative thymocytes progress through to $CD4^+CD8^+$ double positive thymocytes and then onto either CD4 or CD8 single positive cells. DOX treatment virtually depleted both the less mature double positive thymocytes and the mature single positive cells ($CD4^+$ and $CD8^+$) (Table 2). There was no statistically significant reduction in the numbers of $CD4^-/CD8^-$ or macrophages or dendritic cells by DOX.

Figure 3 shows examples of typical 2D gel images of proteins isolated from the thymus of control and DOX-treated mice. PDQuest analysis showed that 12 proteins spots are differentially expressed between the control and DOX-treated mice and these spots are identified as ATP synthase subunit beta, ATP synthase subunit delta, malate dehydrogenase, transaldolase, pyruvate dehydrogenase E1 component subunit b, fatty acid binding protein from adipocytes, fatty acid-binding protein from epidermal, apolipoprotein A-I, HSP70, proteasome subunit beta type 10, cathepsin D, ferritin light chain 1, Isoform 2 of tetratricopeptide repeat protein 38, Rho GDP-dissociation inhibitor 1, annexin A5, actin cytoplasmic 1, tubulin beta-2B

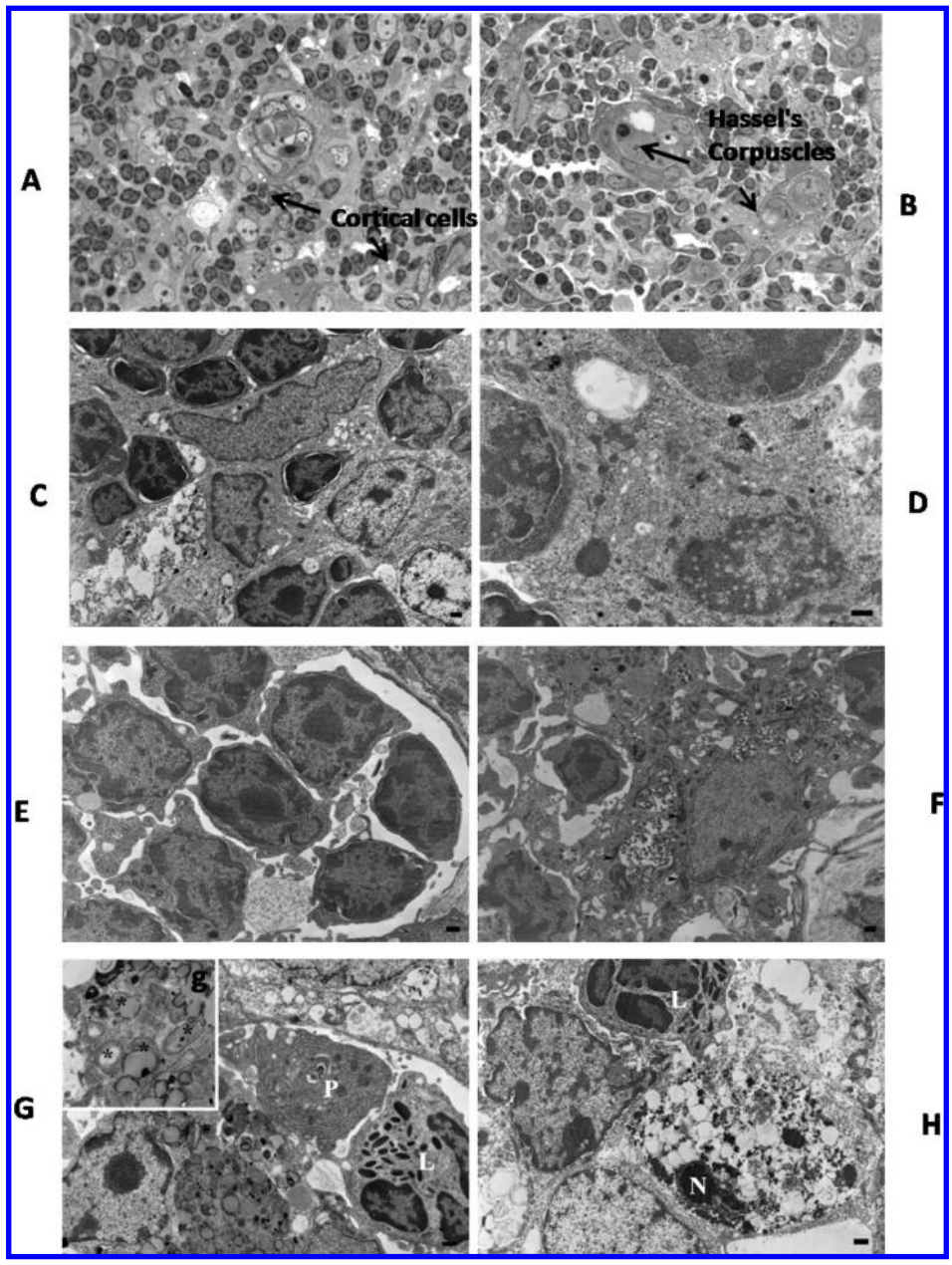

Figure 2. Thymus cytoarchitecture of controls (A) and mice treated with doxorubicin (B) showing increased lipid laden cells in the latter. By electron microscopy, the basic feature of the control mice illustrating the thymocytes, lymphocytes, and macrophages are shown (C and D). The DOX treatment effects illustrated include the continued lymphopoiesis (E), the epithelial thymocyte with tonofilaments and desmosomes (F), the lipid droplet laden large thymocyte (G, inset), the mitochondrial change (G), and a frank degenerative cell (H). Magnification of the images are 1000× and scale bars = 1 μm. See result section for more details.

Table 2. The Number of total CD4/CD8 Subsets and CD 11c, CD 11b, and CD 19 per Whole Thymus of Control and DOX-Treated Mice

	number of thymocytes ± SD ($\times 10^{-7}$)		
phenotypes	control	DOX	*P*-values
$CD4^-$ $CD8^-$	1.8 ± 0.6	0.8 ± 0.7	NS[a]
$CD4^-$ $CD8^+$	2.6 ± 2.0	0.18 ± 0.2	<0.05
$CD4^+$ $CD8^-$	4.4 ± 1.8	0.63 ± 0.8	<0.05
$CD4^+$ $CD8^+$	41.4 ± 19.0	0.2 ± 0.2	<0.05
Dendritic cell (CD 11c)	0.2 ± 0.1	0.01 ± 0.01	<0.05
Macrophage (CD 11b)	0.2 ± 0.1	0.02 ± 0.01	NS[a]

[a] NS = no significant difference.

chain, tubulin alpha-1A chain, and Peripherin with MS and are labeled in Figure 3 and listed in Tables 3 and 4. Figure 4 shows expanded images of selected protein spots which clearly showed the differential levels of proteins between control and DOX-treated groups. The locations of most proteins spots agree with reported p*I* and MW values; however, in some cases, spots differ due likely to protein modifications, fragments, or degradation products that directly influence the net charge and MW of the protein (Table 3). In Table 4, identified differentially expressed proteins are grouped based on their function.

Discussion

The thymus undergoes age-related progressive involution characterized by a decrease in thymic weight, decreased thymic lymphopoiesis, disrupted thymic architecture, decreased numbers of cortical thymocytes, and gradual replacement of epi-

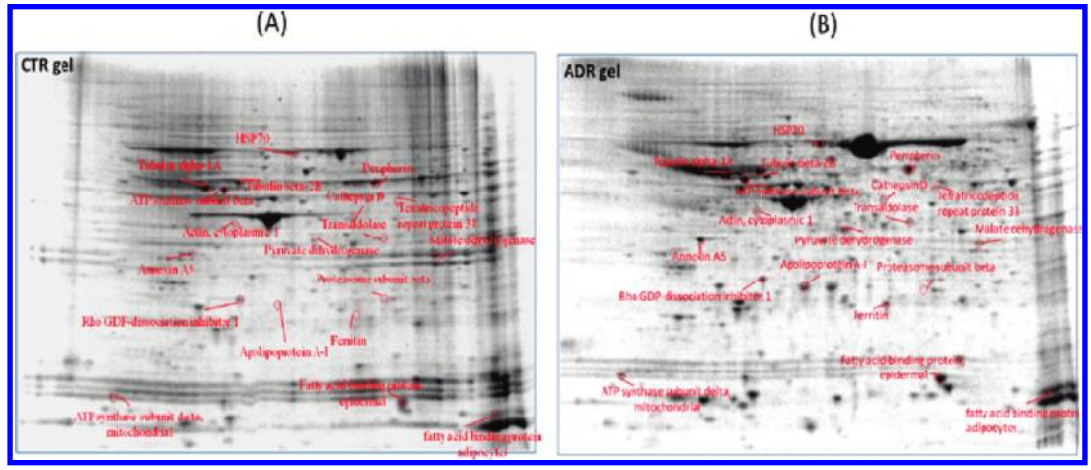

Figure 3. Representative 2D gels from thymus of saline- (A) and doxorubicin-treated mice (B), respectively, showing geographical location of proteins on 2D gel identified by mass spectrometry that showed differences in expression as a result of ip DOX. Spots that showed a significant difference in expression levels are boxed and labeled with the corresponding protein identity ($n = 6$).

Table 3. Proteomic Identification of Differentially Expressed Proteins in Thymus of Mice Treated with Doxorubicin

protein identified	accession number[a]	MW (kDa)	p*I*	peptides (hits)[b]	probability[c]
ATP synthase subunit beta, mitochondrial	P56480	56.26	6.0	12(12)	3e-010
ATP synthase subunit delta, mitochondrial	Q9D3D9	17.59	4.8	2(7)	2e-010
Malate dehydrogenase, cytoplasmic	P14152	36.48	6.1	7(27)	9e-006
Transaldolase	Q93092	37.36	6.6	2(3)	7e-008
Pyruvate dehydrogenase E1 component subunit b	Q9D051	38.91	6.4	1(1)	4e-009
Fatty acid binding protein, adipocytes	P04117	14.64	8.7	3(3)	4e-010
Fatty acid-binding protein, epidermal	Q05816	15.12	6.1	5(64)	0.0002
Apolipoprotein A-I	Q00623	30.56	5.5	2(2)	5e-011
HSP70	P16627	70.59	5.8	1(1)	6e-011
Proteasome subunit beta type 10	O35955	29.04	6.4	2(2)	1e-006
Cathepsin D	P18242	44.92	6.7	4(11)	1e-015
Ferritin light chain 1	P29391	20.76	5.6	3(7)	2e-008
Isoform 2 of Tetratricopeptide repeat protein 38	A3KMP2-2	31.56	5.8	3(4)	9e-006
Rho GDP-dissociation inhibitor 1	Q99PT1	23.39	4.9	6(10)	2e-009
Annexin A5	P48036	35.73	4.6	10(10)	2e-010
Actin, cytoplasmic 1	P60710	41.71	5.1	2(3)	8e-010
Tubulin beta-2B chain	Q9CWF2	49.92	4.69	6(8)	6e-010
Tubulin alpha-1A chain	P68369	50.10	4.81	9(9)	1e-009
Isoform 5 g of Peripherin	P15331-1	54.23	5.29	2(13)	5e-006

[a] The protein accession number found in the Swiss-Prot (mouse) database. [b] The number of peptide sequences identified by ESI−MS/MS. The total number of peptide hits is indicated in parentheses, including multiple hits across different charge states. [c] The probability associated with a false protein identification using the SEQUEST search algorithm.

thelial reticular cells by fat and connective tissue. Thymocytes in the aged thymus have been shown to have altered proliferation and apoptosis.[23] In the present study, we observed that DOX treatment to young animals leads to a decrease in the thymus weight and lymphopoiesis (Tables 1, 2) which correlated well with the decreased number of thymic cells as revealed by histology (Figure 2). Thymic involution is associated with a gradual decline in the size of thymus and also alterations in the intrathymic T-cell development.[24] We measured by flow cytometric analysis the T-cell differentiation of control and DOX-treated thymus in order to evaluate if DOX induced early involution (Table 2). DOX treatment had a significant effect on both the less mature double positive thymocytes and the mature single positive (SP) cells ($CD4^+$ and $CD8^+$); however, $CD4^+$ $CD8^+$ (DP) thymocytes are more sensitive to DOX treatment than $CD4^+$ or $CD8^+$ single positive (SP) thymocytes. Previous study showed that DP cells are more sensitive to glucocorticoid and radiation-induced apoptosis compared to either $CD4^+$ and $CD8^+$ SP cells.[25,26] Further, macrophage and dendritic cells did not show any statistically significant reduction in the number suggesting that they are less vulnerable to DOX-treatment. However, the mechanism of DP cells sensitivity is not clearly understood.

DOX-treated thymus showed increased number of Hassall's corpuscles (HC) that play an important role in the removal of apoptotic cells, in addition to other functions. Further, several studies also suggest that HC may play a role in the appearance of natural regulatory T-cells (Tregs) in human thymic medulla by secreting thymic hormones and promoting dendritic cells to positively select natural Tregs (a subset of thymic B-cells). Hence, the appearance of large number of HC in the DOX-treated thymus can be considered as an augmentation of protective mechanisms to attempt to prevent DOX-induced toxicity and clearance of the dead cells.

Much of the metabolic decline in the thymus can be attributed to age involution that, in rodents, start at about 4 months and slowly progresses during the lifetime of the animal. DOX treatment leads to early senescence of thymus. Proteomics analysis in this study led to the identification of a number of proteins whose expressions are altered upon DOX treatment.

Table 4. Functional Classification of Proteomics Identified Differentially Expressed Proteins in Thymus of Mice Treated with Doxorubicin[a]

proteins	*p*-value	DOX/CTR	functions
ATP synthase subunit beta, mitochondrial	0.007	0.54*	energy metabolism
ATP synthase subunit delta, mitochondrial	0.03	0.63*	energy metabolism
Malate dehydrogenase, cytoplasmic	1.79×10^{-7}	3.67	energy metabolism
Transaldolase	0.006	3.24	energy metabolism
Pyruvate dehydrogenase E1 component subunit b	0.03	1.75	energy metabolism
Fatty acid binding protein, adipocytes	0.01	3.51	fatty acid carriers
Fatty acid-binding protein, epidermal	0.01	1.70	fatty acid carriers
Apolipoprotein A-I	0.008	3.04	lipid metabolism
HSP70	0.0002	3.70	chaperon
Proteasome subunit beta	0.005	0.42*	protein degradation
Cathepsin D	0.003	1.57	protein degradation
Ferritin light chain 1	0.007	1.99	iron storage/stress response
Isoform 2 of Tetratricopeptide repeat protein 38	0.01	2.84	immune system
Rho GDP-dissociation inhibitor 1	0.004	2.20	cell signaling
Annexin A5	0.01	2.24	apoptosis
Actin, cytoplasmic 1	0.02	1.80	structure
Tubulin beta-2B chain	0.02	2.88	structure
Tubulin alpha-1A chain	0.003	1.92	structure
Isoform 5 g of Peripherin	0.0003	3.32	structure

[a] The levels of protein alterations are expressed as the ratio of DOX to control protein levels. '*' indicates the proteins that showed decreased protein levels.

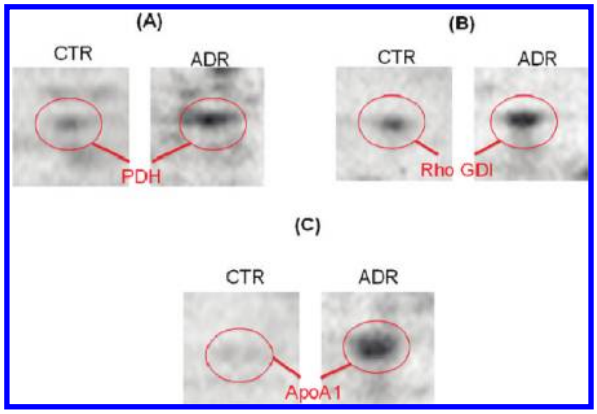

Figure 4. Representative enlarged images of selected spots from control (CTR) and doxorubicin (DOX)-treated mice thymus showing the altered expression of proteins. Panel A represents pyruvate dehydrogenase (PDH), panel B represents Rho GDP-dissociation inhibitor 1 (Rho GDI), and panel C represents APoA1.

These proteins are categorized in Table 4 based on their functions: energy metabolism, lipid metabolism, proteins degradation, chaperon, cell structure, apoptosis, cell signaling, iron storage, and immune response. The functional role of each of the identified proteins is discussed below with emphasis on thymus involution.

Energy Metabolism. A number of thymic proteins related with energy metabolism were found to be affected in DOX-treated mice. These proteins includes ATP synthase (ATPase), pyruvate dehydrogenase (PDH), transaldolase (TAL), and malate dehydrogenase (MDH). Previous studies showed that decline in the metabolic activity in the thymus is related to the thymus involution which starts at about 4 months of mice age and slowly progresses during the lifetime of the animal. Further, the activities of glucose metabolizing enzymes in thymus have been shown to have decreased activity which is age-dependent. The glycolytic pathway of glucose metabolism has been shown to have age-related significant decreases in enzyme activity.[27]

ATPase protein levels were found to be significantly decreased in thymus of animals treated with DOX. ATPase is a mitochondrial enzyme that plays a key role in energy production. ATPase is formed by two complexes, F0 within the membrane and F1 above the membrane, inside the matrix of the mitochondria. The F1 complex contains the catalytic core that synthesizes/hydrolyses ATP, while the F0 complex forms the membrane-spanning pore. In F-ATPases, three copies each of the alpha and beta subunits form the catalytic core of the F1 complex, while the remaining F1 subunits (gamma, delta, epsilon) form part of the stalks.[28] ATPase, by complex rotational movements of its subunits, couples the proton gradient generated by the respiratory chain which promotes ATP synthesis and release.[29] Having a decreased expression of ATPase would lead to reduced production of ATP thereby affecting the normal cellular functions which may lead to loss of thymus cells.

PDH protein levels were found to be significantly increased in thymus of animals treated with DOX. PDH is a mitochondrial enzyme complex that catalyzes the oxidative decarboxylation of pyruvate to acetyl CoA, NADH, and CO_2, making this protein the key link between glycolysis and the citric acid cycle.[30] The increase in the levels of PDH might be a compensatory response to increase the ATP production due to decrease levels of ATPases.

TAL protein level was identified as significantly increased in thymus of animals treated with DOX. TAL is an enzyme of the nonoxidative phase of the pentose phosphate pathway (PPP). TAL catalyzes the reversible transfer of a three-carbon ketol unit from sedoheptulose 7-phosphate to glyceraldehyde 3-phosphate to form erythrose 4-phosphate and fructose 6-phosphate. This enzyme, together with transketolase, provides a link between the glycolytic and pentose-phosphate pathways.[31] TAL has been proposed as one of a rate-limiting enzyme of the PPP, playing a key role in the control of the metabolic network that regulates cell survival and differentiation.[32] The increase in levels of TAL might also be a compensatory response to increase the ATP production due to decrease levels of ATPases.

MDH protein level was identified as significantly increased in thymus of animals treated with DOX. MDH is involved in the malate-aspartate shuttle catalyzing the reversible oxidation

of malate to oxaloacetate by NAD^+ in the TCA cycle, also producing ATP from ADP. MDH is located within the mitochondrial matrix linking glycolysis to mitochondrial respiration. This protein transfers NADH across the mitochondrial membrane to respiratory complex I.[33] Previous studies showed that glucose metabolism results in increased proliferating compared to resting thymocytes.[34]We speculate that the up-regulation of MDH may be a compensatory mechanism for reduced level of ATP synthase, downstream in the electron transport chain.

We hypothesize that the loss of a number of cortical cells together with the decrease in the levels of protein ATPase leads to up-regulation of a number of the other proteins that are energy related as discussed above. The maintenance of normal ATP levels in the cell is critical for cell survival and to carry out normal cellular activities. A decrease in ATP production leads to alteration in ATP dependent protein functions, such as Na^+/K^+ ATPase, which are important in maintaining the ion-gradients across the cell, thereby affecting the cell survival, the loss of which leads to cell death. The loss of cortical cells seen after DOX treatment could be the DOX-induced effect on the loss of cellular energetics. However, further studies are needed to confirm this hypothesis.

Lipid Metabolism, Fatty Acyls Carriers. One of the characteristic features of senescence of the thymus is loss of thymocytes and increase deposition of fat. In the current study, we found that apolipoprotein A 1 (ApoA1) and fatty acid binding proteins (FABPs) levels are significantly increased compared to control mice thymus consistent with the notion that DOX induces thymus senescence.

ApoA1 is the major apolipoprotein associated with high-density lipoprotein (HDL) and plays an important role in the process of reverse cholesterol transport. This process is involved in the transport of cholesterol from peripheral tissues to the liver for processing, thereby eliminating excess cholesterol from the body. In this process, apoA1 acts as a cofactor for lecithin cholesterol acyltransferase.[35,36] ApoA1 deficiency in humans leads to a phenotype of low plasma HDL levels and premature atherosclerosis.[37] ApoA1 knockout mice show a marked reduction in plasma HDL levels that is repeated in levels of total plasma cholesterol.[38,39] Increased Apo A-1 levels has been suggested to have anti-inflammatory activities.[40]

FABPs are soluble proteins with binding ability for unsaturated long chain fatty acids. The possible roles of FABPs include promotion of cellular uptake of fatty acids and their utilization, compartmentalization of intracellular fatty acid storage, modulation of enzyme activities, and protection of enzymes against detrimental effects of fatty acids. These FABPs were originally named according to the tissue of their first isolation such as epidermal (E), heart (H), brain (B), liver (L), intestine (I), and adipocyte (A) FABPs. Recent study reported that the thymus is rich in E-FABP suggesting that E-FABP is involved in a function essential to the thymic epithelial stromal cells.[41] The thymic epithelial stromal cells are involved in some regulation of thymic immune responses through E-FABP-mediated metabolic processes of fatty acids such as regulation in production of potent thymic lipid-mediators such as prostaglandins.[41] Degeneration of thymus tissues at old age is associated with a substitution of thymocytes by adipocytes, indicating the presence of neo-generation mechanisms of new adipose tissue.[42] A-FABP is a predominant cytosolic protein in mature adipocytes. This protein may be an important regulator of systemic insulin sensitivity and lipid and glucose metabolism. Mice deficient in A-FABP are protected from development of hyperinsulinemia and hyperglycemia. Indeed, in apolipoprotein E-deficient mice, ablation of the A-FABP gene conferred remarkable protection against atherosclerosis and insulin resistance.[43] A-FABP is present also in macrophages where it modulates inflammatory cytokine production and cholesterol ester accumulation. A-FABP expression in macropages can be induced by oxidized LDL and by toll-like receptor agonists.[43] The increase in the FABP may lead to increase in the fat deposition, one of the hallmarks of thymus involution. Our ultrastructural demonstration of the increase lipid droplets in thymic epithelial cell also suggests that DOX affects the thymic development and consequently leads to thymus senescence.

Proteins Degradation and Chaperones. Cathepsin D (CD) protein level was found to be significantly increased in thymus of animals treated with DOX. CD is an aspartic proteinase which is ubiquitously expressed in lysosomes of most eukaryotic cells contributing to lysosomal proteolysis. CD has also been implicated in regulation of cell proliferation and apoptosis signaling pathways. Increased CD levels are associated with metastatic potential in some cancers, possibly reflecting the increased metabolism of these cells, or due to a role in extracellular matrix degradation. CD has been shown to be in the lysosomes and in the endosomes of macrophages, suggesting its involvement in proteolytic processing of foreign antigens and invariant chain.[44] CD deficiency conferred a lethal phenotype with mice showing profound atrophy of lymphoid tissue such as thymus and spleen and progressive atrophy of the intestinal mucosa, suggesting essential functions of CD in tissue homeostasis.[45,46] Hence, increased levels of CD found in the current study possibly indicate an increased rate of metabolism in the surviving cells (possibly to compensate for decreased ATP synthase) or a signal of apoptosis in the DOX-treated mice thymus.

The proteasome constitutes the central proteolytic component of the highly conserved ubiquitin−proteasome system that is responsible for mediating the degradation of a vast array of oxidized, misfolded, and aggregated proteins.[47] The proteolytic core of the proteasome, referred to as the 20S proteasome, is composed of multiple α- and β-subunits. Additional cap-like protein complexes, referred to as the 11S and 19S proteasomes, can bind to the 20S proteasome resulting in the formation of the 26S proteasome.[48] The proteasome is required for the maintenance and regulation of basic cellular processes, including differentiation, proliferation, cell cycling, gene transcription, apoptosis, and the generation of antigenic peptides presented by major histocompatibility complex (MHC) class I molecules.[47] Increasing evidence suggests that the activity and composition of the proteasome can be altered in immune cells in response to inflammatory stimuli in order to maintain proper immune function.[48] Moreover, it has been shown that there is a decrease in proteasome activity in apoptotic thymocytes.[49] Therefore, decreased levels of proteasome subunit beta in thymus of mice treated with DOX may lead to increase accumulation of damaged proteins which may eventually lead to increased loss of cells, as observed by loss of cortical cells (Figure 2).

Heat shock protein 70 (HSP 70) protein level was found to be significantly increased in thymus of animals treated with DOX. HSP 70 is the major heat-inducible chaperone protein that exerts a cytoprotective effect under a number of different conditions. HSP 70 prevents protein aggregation, assists in the refolding of damaged proteins, and chaperones nascent polypeptides along ribosomes. Moreover, HSP 70 is also involved in the ubiquitin−proteasome pathway.[50] Transgenic mice ex-

pressing the inducible human HSP 70 developed thymic hypoplasia and immunodeficiency due to the lack of mature T cells in the thymus and the periphery.[51] According to Selye's theory on stress response, the body reacts in response to different stress inducers with a typical stress syndrome characterized by thymic involution.[52] Therefore, elevated HSP70 following DOX is consistent with the fact that the DOX treatement leads to protein misfolding in thymus cells leading to altered cellular functions and eventually to immunosenescence.

Cell Structure. Among other moieties, the cell cytoskeleton consists of microtubules and microfilaments that participate in processes that require changes in the shape of the cell and transport of materials. There are three interconnected filament systems in eukaryotic cells: microfilaments consisting of actin, microtubules made from α/β-tubulin subunits, and intermediate filaments.

Actin is a principal protein playing a central role in maintaining cellular integrity, morphology, and the structure of the plasma membrane. Actin is the monomeric subunit of microfilaments. Actin participates in many important cellular processes including cell motility, cell division and cytokinesis, vesicle and organelle movement, cell signaling, and the establishment and maintenance of cell junctions and cell shape.

Tubulin is a core protein of microtubules, which play a role in cytoskeletal maintenance and transport of membrane-bound organelles. Tubulin alpha and beta heterodimers represent the major components. Tubulin binds 2 mol of GTP, one at an exchangeable site on the beta chain and one at a nonexchangeable site on the alpha chain.

Peripherin is one of the neuronal intermediate filament proteins (IFPs) expressed in mammals.[53] Peripherin appears during development in motoneurons, neural crest-derived and some placode-derived neurons. Peripherin expression peaks during the axonal growth phase, but decreases later during postnatal development. The levels of peripherin protein are considerably up-regulated after injury.[54] A tight link between epithelial and neural cell lineages has been suggested in thymus. Several studies described the coexistence of neural crest-derived cells together with distinct cell lineages in thymic medulla and the expression of a number of neuronal markers and neuropeptides in both thymic epithelium and stromal.[55] Taken together, dysregulation of the structural proteins may lead to alteration in normal cellular functions leading to cell death and consequently to immunosenescence. Lastly, although the study duration of DOX exposure is relatively brief, the mitochondrial degeneration seen in many thymocytes (Figure 2G) is consistent with the known mitochondrial toxicity of DOX.

Apoptosis, Cell Signaling, Iron Storage, and Immune Response. The annexins are a family of membrane binding proteins that share structural properties and biological activities associated with membrane related processes. Annexin A5 binds in a calcium-dependent and reversible manner to PtdSer-expressing membranes. Annexin A5 potentially plays a role in various biochemical and cellular processes occurring on membranes in which PtdSer is expressed on the outer lamella. It has been reported that annexin A5 inhibits apoptotic body formation by applying a physical constraint on the plasma membrane and inhibiting the apoptotic program.[56] Munoz et al. proposed that annexin A5 plays a role in the modulation of the immune system by inhibiting phagocytosis of apoptotic and necrotic cells.[57] Hence, DOX-induced changes could be a compensatory response to protect the cells and consequently immunosenescence.

The Rho-family specific GDP-dissociation inhibitor (Rho GDI) forms complexes with Rho proteins in the cytosol of mammalian cells. Rho GDIs block activation of Rho proteins by sequestering the GDP-bound Rho proteins in the cytosol, thereby inhibiting the exchange of GDP to GTP of Rho proteins. Moreover, they target Rho proteins to specific signaling complexes at the plasma membrane and protect Rho proteins from proteolytic degradation by forming stable complexes in the cytosol.[58] Rho GDI are involved in the control of cell morphology and motility in untransformed cells. The increase in Rho GDI could be a compensatory response to the altered signal transduction in the thymus of DOX-treated mice, which may eventually lead to immunosenescence.

Ferritin is the major intracellular iron storage protein and is composed of 24 subunits of the heavy and light chains. Variation in ferritin subunit composition may affect the rates of iron uptake and release in different tissues. A major function of ferritin is the storage of iron in a soluble nontoxic, readily available state. Ferritin is important for iron homeostasis and plays a key role in delivery of iron to cells.[59] We hypothesize that cell loss triggered by DOX-treatment may lead to increase release of iron from the damaged protein, an the increase in the levels of ferritin could be a protective mechanism to prevent thymus involution.

Tetratricopeptide repeat protein 38 is a novel immunophilin homologue that contains a three-unit tetratricopeptide repeat and a consensus leucine zipper. Immunophilins comprise a family of proteins that serve as receptors for immunosuppressant drugs such as cyclosporin A. Immunophilins are thought to interact with a several intracellular signal transduction systems especially those related to calcium and phosphorylation. Immunophilins are also important therapeutic targets for induced immunosuppression of T-cells in association with organ transplantation.[60] We hypothesize that the increase in Tetratricopeptide repeat protein 38 could be a compensatory response to decrease immunity reported in patients treated by DOX, making the cancer patients more vulnerable to infection.

Conclusion

The ip DOX treatment clearly affected the thymus cytoarchitecture. Large increase of the vesiculated, lipid laden epithelial thymocytes with mitochondria degeneration may be the morphological cornerstone of the molecular observations presented. Further, we identified a number of proteins that were differentially regulated in DOX-treated mice thymus, which suggests that DOX treatment leads to early senescence of thymus. Further studies are needed to understand the mechanism of DOX-induced senescence and to prevent DOX-induced side effects in cancer treatment. In addition, better insights into DOX effects on thymus will also help in developing a strategy to delay or prevent age-induced thymus involution and promote a more healthy life.

Acknowledgment. This work was supported in part by funds from the University of Kentucky Markey Cancer Center.

References

(1) Cummings, J.; Anderson, L.; Willmott, N.; Smyth, J. F. The molecular pharmacology of doxorubicin in vivo. *Eur. J. Cancer* **1991**, *27* (5), 532–5.

(2) Fornari, F. A.; Randolph, J. K.; Yalowich, J. C.; Ritke, M. K.; Gewirtz, D. A. Interference by doxorubicin with DNA unwinding in MCF-7 breast tumor cells. *Mol. Pharmacol.* **1994**, *45* (4), 649–56.
(3) Tanaka, M.; Yoshida, S. Mechanism of the inhibition of calf thymus DNA polymerases alpha and beta by daunomycin and adriamycin. *J. Biochem.* **1980**, *87* (3), 911–8.
(4) Chuang, R. Y.; Chuang, L. F. Inhibition of chicken myeloblastosis RNA polymerase II activity by adriamycin. *Biochemistry* **1979**, *18* (10), 2069–73.
(5) Bachur, N. R.; Gordon, S. L.; Gee, M. V. Anthracycline antibiotic augmentation of microsomal electron transport and free radical formation. *Mol. Pharmacol.* **1977**, *13* (5), 901–10.
(6) Deres, P.; Halmosi, R.; Toth, A.; Kovacs, K.; Palfi, A.; Habon, T.; et al. Prevention of doxorubicin-induced acute cardiotoxicity by an experimental antioxidant compound. *J. Cardiovasc. Pharmacol.* **2005**, *45* (1), 36–43.
(7) DeAtley, S. M.; Aksenov, M. Y.; Aksenova, M. V.; Jordan, B.; Carney, J. M.; Butterfield, D. A. Adriamycin-induced changes of creatine kinase activity in vivo and in cardiomyocyte culture. *Toxicology* **1999**, *134* (1), 51–62.
(8) Jungsuwadee, P.; Cole, M. P.; Sultana, R.; Joshi, G.; Tangpong, J.; Butterfield, D. A.; et al. Increase in Mrp1 expression and 4-hydroxy-2-nonenal adduction in heart tissue of Adriamycin-treated C57BL/6 mice. *Mol. Cancer Ther.* **2006**, *5* (11), 2851–60.
(9) Joshi, G.; Sultana, R.; Tangpong, J.; Cole, M. P.; St Clair, D. K.; Vore, M.; et al. Free radical mediated oxidative stress and toxic side effects in brain induced by the anti cancer drug adriamycin: insight into chemobrain. *Free Radical Res.* **2005**, *39* (11), 1147–54.
(10) Tangpong, J.; Cole, M. P.; Sultana, R.; Estus, S.; Vore, M.; St Clair, W.; et al. Adriamycin-mediated nitration of manganese superoxide dismutase in the central nervous system: insight into the mechanism of chemobrain. *J. Neurochem.* **2007**, *100* (1), 191–201.
(11) Cardoso, S.; Santos, R. X.; Carvalho, C.; Correia, S.; Pereira, G. C.; Pereira, S. S.; et al. Doxorubicin increases the susceptibility of brain mitochondria to Ca(2+)-induced permeability transition and oxidative damage. *Free Radical Biol. Med.* **2008**, *45* (10), 1395–402.
(12) Yeh, Y. C.; Liu, T. J.; Wang, L. C.; Lee, H. W.; Ting, C. T.; Lee, W. L.; et al. A standardized extract of Ginkgo biloba suppresses doxorubicin-induced oxidative stress and p53-mediated mitochondrial apoptosis in rat testes. *Br. J. Pharmacol.* **2009**, *156* (1), 48–61.
(13) Qin, X. J.; He, W.; Hai, C. X.; Liang, X.; Liu, R. Protection of multiple antioxidants Chinese herbal medicine on the oxidative stress induced by adriamycin chemotherapy. *J. Appl. Toxicol.* **2008**, *28* (3), 271–82.
(14) Aluise, C. D.; St Clair, D.; Vore, M.; Butterfield, D. A. In vivo amelioration of adriamycin induced oxidative stress in plasma by gamma-glutamylcysteine ethyl ester (GCEE. *Cancer Lett.* **2009**, *282* (1), 25–9.
(15) Munoz-Castaneda, J. R.; Muntane, J.; Munoz, M. C.; Bujalance, I.; Montilla, P.; Tunez, I. Estradiol and catecholestrogens protect against adriamycin-induced oxidative stress in erythrocytes of ovariectomized rats. *Toxicol. Lett.* **2006**, *160* (3), 196–203.
(16) Wagner, W. M.; Ouyang, Q.; Sekeri-Pataryas, K.; Sourlingas, T. G.; Pawelec, G. Basic biology and clinical impact of immunosenescence. *Biogerontology* **2004**, *5* (1), 63–6.
(17) Tarazona, R.; Solana, R.; Ouyang, Q.; Pawelec, G. Basic biology and clinical impact of immunosenescence. *Exp. Gerontol.* **2002**, *37* (2−3), 183–9.
(18) Ongradi, J.; Stercz, B.; Kovesdi, V.; Vertes, L. Immunosenescence and vaccination of the elderly, I. Age-related immune impairment. *Acta Microbiol. Immunol. Hung.* **2009**, *56* (3), 199–210.
(19) Huang, Q. A.; Christopher, D.; Joshi, G.; Sultana, R.; St. Clair, D.; Markesbery, K.; William, R.; Butterfield, D. A. In vivo protection by N-acetyl-L-cysteine against oxidative stress in brain in human double mutant APP/PS-1 knock-in mice: Towards therapeutic modulation of mild cognitive impairment (MCI). *J. Neurosci. Res.* **2010**, *88* (12), 2618–29.
(20) Sultana, R.; Boyd-Kimball, D.; Poon, H. F.; Cai, J.; Pierce, W. M.; Klein, J. B.; et al. Redox proteomics identification of oxidized proteins in Alzheimer's disease hippocampus and cerebellum: an approach to understand pathological and biochemical alterations in AD. *Neurobiol. Aging* **2006**, *27* (11), 1564–76.
(21) Sultana, R.; Boyd-Kimball, D.; Cai, J.; Pierce, W. M.; Klein, J. B.; Merchant, M.; et al. Proteomics analysis of the Alzheimer's disease hippocampal proteome. *J. Alzheimer's Dis.* **2007**, *11* (2), 153–64.
(22) Sultana, R.; Reed, T.; Perluigi, M.; Coccia, R.; Pierce, W. M.; Butterfield, D. A. Proteomic identification of nitrated brain proteins in amnestic mild cognitive impairment: a regional study. *J. Cell. Mol. Med.* **2007**, *11* (4), 839–51.
(23) Gui, J.; Zhu, X.; Dohkan, J.; Cheng, L.; Barnes, P. F.; Su, D. M. The aged thymus shows normal recruitment of lymphohematopoietic progenitors but has defects in thymic epithelial cells. *Int. Immunol.* **2007**, *19* (10), 1201–11.
(24) Chen, Y. T.; Chen, F. L.; Kung, J. T. Age-associated rapid and Stat6-independent IL-4 production by NK1-CD4 + 8- thymus T lymphocytes. *J. Immunol.* **1999**, *163* (9), 4747–53.
(25) Ryan, J. A.; Brunelle, J. K.; Letai, A. Heightened mitochondrial priming is the basis for apoptotic hypersensitivity of CD4+ CD8+ thymocytes. *Proc. Natl. Acad. Sci. U.S.A.* **2010**, *107* (29), 12895–900.
(26) Grillot, D. A.; Merino, R.; Nunez, G. Bcl-XL displays restricted distribution during T cell development and inhibits multiple forms of apoptosis but not clonal deletion in transgenic mice. *J. Exp. Med.* **1995**, *182* (6), 1973–83.
(27) Dieter, M. P.; Wilson, R.; Birnbaum, L. S. Age-related changes in glucose metabolizing enzymes in spleen, thymus, and pulmonary lavage cells from F344 rats. *Mech. Ageing Dev.* **1984**, *26* (2−3), 253–63.
(28) Leyva, J. A.; Bianchet, M. A.; Amzel, L. M. Understanding ATP synthesis: structure and mechanism of the F1-ATPase (Review. *Mol. Membr. Biol.* **2003**, *20* (1), 27–33.
(29) Junge, W.; Lill, H.; Engelbrecht, S. ATP synthase: an electrochemical transducer with rotatory mechanics. *Trends Biochem. Sci.* **1997**, *22* (11), 420–3.
(30) Zaidan, E.; Sheu, K. F.; Sims, N. R. The pyruvate dehydrogenase complex is partially inactivated during early recirculation following short-term forebrain ischemia in rats. *J. Neurochem.* **1998**, *70* (1), 233–41.
(31) Verhoeven, N. M.; Huck, J. H.; Roos, B.; Struys, E. A.; Salomons, G. S.; Douwes, A. C.; et al. Transaldolase deficiency: liver cirrhosis associated with a new inborn error in the pentose phosphate pathway. *Am. J. Hum. Genet.* **2001**, *68* (5), 1086–92.
(32) Grossman, C. E.; Qian, Y.; Banki, K.; Perl, A. ZNF143 mediates basal and tissue-specific expression of human transaldolase. *J. Biol. Chem.* **2004**, *279* (13), 12190–205.
(33) Poon, H. F.; Vaishnav, R. A.; Butterfield, D. A.; Getchell, M. L.; Getchell, T. V. Proteomic identification of differentially expressed proteins in the aging murine olfactory system and transcriptional analysis of the associated genes. *J. Neurochem.* **2005**, *94* (2), 380–92.
(34) Brand, K. Glutamine and glucose metabolism during thymocyte proliferation. Pathways of glutamine and glutamate metabolism. *Biochem. J.* **1985**, *228* (2), 353–61.
(35) Yang, M.; Lee, H. S.; Pyo, M. Y. Proteomic biomarkers for prenatal bisphenol A-exposure in mouse immune organs. *Environ. Mol. Mutagen.* **2008**, *49* (5), 368–73.
(36) Liu, H. C.; Hu, C. J.; Chang, J. G.; Sung, S. M.; Lee, L. S.; Yuan, R. Y.; et al. Proteomic identification of lower apolipoprotein A-I in Alzheimer's disease. *Dementia Geriatr. Cognit. Disord.* **2006**, *21* (3), 155–61.
(37) Fagan, A. M.; Christopher, E.; Taylor, J. W.; Parsadanian, M.; Spinner, M.; Watson, M.; et al. ApoAI deficiency results in marked reductions in plasma cholesterol but no alterations in amyloid-beta pathology in a mouse model of Alzheimer's disease-like cerebral amyloidosis. *Am. J. Pathol.* **2004**, *165* (4), 1413–22.
(38) Plump, A. S.; Azrolan, N.; Odaka, H.; Wu, L.; Jiang, X.; Tall, A.; et al. ApoA-I knockout mice: characterization of HDL metabolism in homozygotes and identification of a post-RNA mechanism of apoA-I up-regulation in heterozygotes. *J. Lipid Res.* **1997**, *38* (5), 1033–47.
(39) Williamson, R.; Lee, D.; Hagaman, J.; Maeda, N. Marked reduction of high density lipoprotein cholesterol in mice genetically modified to lack apolipoprotein A-I. *Proc. Natl. Acad. Sci. U.S.A.* **1992**, *89* (15), 7134–8.
(40) Bresnihan, B.; Gogarty, M.; FitzGerald, O.; Dayer, J. M.; Burger, D. Apolipoprotein A-I infiltration in rheumatoid arthritis synovial tissue: a control mechanism of cytokine production? *Arthritis Res. Ther.* **2004**, *6* (6), R563–6.
(41) Owada, Y.; Suzuki, R.; Iwasa, H.; Spener, F.; Kondo, H. Localization of epidermal-type fatty acid binding protein in the thymic epithelial cells of mice. *Histochem. Cell Biol.* **2002**, *117* (1), 55–60.
(42) Tinahones, F.; Salas, J.; Mayas, M. D.; Ruiz-Villalba, A.; Macias-Gonzalez, M.; Garrido-Sanchez, L.; et al. VEGF gene expression in adult human thymus fat: a correlative study with hypoxic induced factor and cyclooxygenase-2. *PLoS One* **2009**, *4* (12), e8213.
(43) Xu, A.; Wang, Y.; Xu, J. Y.; Stejskal, D.; Tam, S.; Zhang, J.; et al. Adipocyte fatty acid-binding protein is a plasma biomarker closely associated with obesity and metabolic syndrome. *Clin Chem.* **2006**, *52* (3), 405–13.
(44) Nishishita, K.; Sakai, H.; Sakai, E.; Kato, Y.; Yamamoto, K. Age-related and dexamethasone-induced changes in cathepsins E and

D in rat thymic and splenic cells. *Arch. Biochem. Biophys.* **1996**, *333* (2), 349–58.
(45) Saftig, P.; Hetman, M.; Schmahl, W.; Weber, K.; Heine, L.; Mossmann, H.; et al. Mice deficient for the lysosomal proteinase cathepsin D exhibit progressive atrophy of the intestinal mucosa and profound destruction of lymphoid cells. *EMBO J.* **1995**, *14* (15), 3599–608.
(46) Tulone, C.; Uchiyama, Y.; Novelli, M.; Grosvenor, N.; Saftig, P.; Chain, B. M. Haematopoietic development and immunological function in the absence of cathepsin D. *BMC Immunol.* **2007**, *8*, 22.
(47) Tomaru, U.; Ishizu, A.; Murata, S.; Miyatake, Y.; Suzuki, S.; Takahashi, S.; et al. Exclusive expression of proteasome subunit {beta}5t in the human thymic cortex. *Blood* **2009**, *113* (21), 5186–91.
(48) Ding, Q.; Reinacker, K.; Dimayuga, E.; Nukala, V.; Drake, J.; Butterfield, D. A.; et al. Role of the proteasome in protein oxidation and neural viability following low-level oxidative stress. *FEBS Lett.* **2003**, *546* (2−3), 228–32.
(49) Beyette, J.; Mason, G. G.; Murray, R. Z.; Cohen, G. M.; Rivett, A. J. Proteasome activities decrease during dexamethasone-induced apoptosis of thymocytes. *Biochem. J.* **1998**, *332* (Pt. 2), 315–20.
(50) Di Domenico, F.; Sultana, R.; Tiu, G. F.; Scheff, N. N.; Perluigi, M.; Cini, C.; et al. Protein levels of heat shock proteins 27, 32, 60, 70, 90 and thioredoxin-1 in amnestic mild cognitive impairment: An investigation on the role of cellular stress response in the progression of Alzheimer disease. *Brain Res.* **2010**, *1333*, 72–81.
(51) Lee, W. H.; Park, Y. M.; Kim, J. I.; Park, W. Y.; Kim, S. H.; Jang, J. J.; et al. Expression of heat shock protein 70 blocks thymic differentiation of T cells in transgenic mice. *Immunology* **1998**, *95* (4), 559–65.
(52) Selye, H. A syndrome produced by diverse nocuous agents. 1936. *J. Neuropsychiatry Clin. Neurosci.* **1998**, *10* (2), 230–1.
(53) Portier, M. M.; de Nechaud, B.; Gros, F. Peripherin, a new member of the intermediate filament protein family. *Dev. Neurosci.* **1983**, *6* (6), 335–44.
(54) Terao, E.; Janssens, S.; van den Bosch de Aguilar, P.; Portier, M.; Klosen, P. In vivo expression of the intermediate filament peripherin in rat motoneurons: modulation by inhibitory and stimulatory signals. *Neuroscience* **2000**, *101* (3), 679–88.
(55) Screpanti, I.; Scarpa, S.; Meco, D.; Bellavia, D.; Stuppia, L.; Frati, L.; et al. Epidermal growth factor promotes a neural phenotype in thymic epithelial cells and enhances neuropoietic cytokine expression. *J. Cell Biol.* **1995**, *130* (1), 183–92.
(56) Kenis, H.; van Genderen, H.; Bennaghmouch, A.; Rinia, H. A.; Frederik, P.; Narula, J.; et al. Cell surface-expressed phosphatidylserine and annexin A5 open a novel portal of cell entry. *J. Biol. Chem.* **2004**, *279* (50), 52623–9.
(57) Munoz, L. E.; Frey, B.; Pausch, F.; Baum, W.; Mueller, R. B.; Brachvogel, B.; et al. The role of annexin A5 in the modulation of the immune response against dying and dead cells. *Curr. Med. Chem.* **2007**, *14* (3), 271–7.
(58) Zhao, L.; Wang, H.; Li, J.; Liu, Y.; Ding, Y. Overexpression of Rho GDP-dissociation inhibitor alpha is associated with tumor progression and poor prognosis of colorectal cancer. *J. Proteome Res.* **2008**, *7* (9), 3994–4003.
(59) Li, J. Y.; Paragas, N.; Ned, R. M.; Qiu, A.; Viltard, M.; Leete, T.; et al. Scara5 is a ferritin receptor mediating non-transferrin iron delivery. *Dev. Cell* **2009**, *16* (1), 35–46.
(60) Pedersen, K. M.; Finsen, B.; Celis, J. E.; Jensen, N. A. muFKBP38: a novel murine immunophilin homolog differentially expressed in Schwannoma cells and central nervous system neurons in vivo. *Electrophoresis* **1999**, *20* (2), 249–55.

PR100465M